WP15ER-CPR(17) 17545

M Perne et al.

Local Decay of Residuals in Dual Gradient Method Applied to MPC Studied Using Active Set Approach

Preprint of Paper to be submitted for publication in Proceeding of
14th International Conference on Informatics in Control,
Automation and Robotics (ICINCO)

This work has been carried out within the framework of the EUROfusion Consortium and has received funding from the Euratom research and training programme 2014-2018 under grant agreement No 633053. The views and opinions expressed herein do not necessarily reflect those of the European Commission.

Local Decay of Residuals in Dual Gradient Method Applied to MPC Studied Using Active Set Approach

Matija Perne[1], Samo Gerkšič[1] and Boštjan Pregelj[1]
[1]*Jožef Stefan Institute, Jamova cesta 39, Ljubljana, Slovenia*
{*matija.perne, samo.gerksic, bostjan.pregelj*}*@ijs.si*

Keywords: Model Predictive Control, Gradient Method, Optimization

Abstract: A dual gradient method is used for solving quadratic programs resulting from a model predictive control problem in real-time control context. Evolution of iterates and residuals throughout multiple iterations is studied. The decay of residuals is observed in intervals where the set of active constraints remains constant. Dual residual can be expressed in a base that depends only on the system matrices and the set of active constraints so that the components are decaying independently and uniformly, and their decay rates can be calculated. The calculated decay rates match the rates observed in numerical simulations of MPC control of the AFTI-16 benchmark model.

1 INTRODUCTION

Model predictive control (MPC) is traditionally limited to processes with relatively slow dynamics because of the computational complexity of online optimization (Qin and Badgwell, 2003). In the recent decade, a considerable advance is seen in the field of fast online optimization (Ferreau et al., 2008; Wang and Boyd, 2010; Mattingley et al., 2011; Mattingley and Boyd, 2012; Domahidi et al., 2012; Hartley et al., 2014; Ferreau et al., 2014).

The advantages of MPC appear promising for the implementation of advanced plasma current and shape control in a tokamak fusion reactor (Gerkšič and Tommasi, 2014). In particular, we are focusing on fast online implementations of first-order methods adapted for use with MPC (Richter, 2012; Giselsson, 2013; Kouzoupis, 2014; Giselsson and Boyd, 2015; Patrinos et al., 2015) Generally, they may require a considerable number of iterations to converge to the optimum, compared to active-set or interior-point methods. However, each iteration is relatively simple, so that the implementation is possible in restricted hardware, and the methods were found to be computationally efficient for the computation of quadratic programs arising from MPC where a relatively low accuracy of the solution is sufficient.

In principle, we are highly interested in complexity certification, that the solution with an acceptable tolerance can be found in a certain maximum number of iterations (limited time). However, practically useful certification is currently not available with any of the relevant methods for practical cases of control problems with state constraints. Despite this, a number of methods typically converge reasonably fast, hence our interest in the practical rates of decay of residuals.

In this work, we examine the rates of decay observed with the dual gradient method. In our MPC simulations, we have observed very different decay rates, which we found to be in close relation with the sets of constraints which were active in the corresponding intervals. We present a theoretical expression for the decay rates in intervals with a constant set of active constraints, which can be computed from the system matrices and the set of constraints. The result is illustrated with MPC application to the AFTI-16 control benchmark (Kapasouris et al., 1990; Giselsson, 2013).

2 MPC

Optimal control of a linear system with constraints and with quadratic cost in discrete time with finite horizon N (Giselsson, 2013) is investigated. The dynamics is:

$$\mathbf{x}(t+1) = \mathbf{A}\mathbf{x}(t) + \mathbf{B}\mathbf{u}(t), \qquad (1)$$

where t is the time index, $\mathbf{x}$ is the system state, $\mathbf{u}$ is system input, matrices $\mathbf{A}$ and $\mathbf{B}$ describe the system

dynamics. Value of $\mathbf{x}(0)$ is known. Possible system states and inputs are constrained to $\mathbf{x} \in \mathcal{X}, \mathbf{u} \in \mathcal{U}$ where $\mathcal{X} \subset \mathbb{R}^l$, $\mathcal{U} \subset \mathbb{R}^m$ are polyhedra. A cost function is defined:

$$J = \frac{1}{2} \sum_{k=0}^{N} \left(\mathbf{x}_k - \mathbf{x}_{\text{ref}}\right)^{\mathrm{T}} \mathbf{Q} \left(\mathbf{x}_k - \mathbf{x}_{\text{ref}}\right) + \left(\mathbf{u}_k - \mathbf{u}_{\text{ref}}\right)^{\mathrm{T}} \mathbf{R} \left(\mathbf{u}_k - \mathbf{u}_{\text{ref}}\right) \tag{2}$$

where $\mathbf{Q}$ and $\mathbf{R}$ are symmetric positive semidefinite cost matrices. Constant vectors $\mathbf{x}_{\text{ref}}$, $\mathbf{u}_{\text{ref}}$ are reference values.

The control is obtained by minimizing the cost function J with respect to constraints

$$\begin{aligned} J^* = \min_{\mathbf{x}_0,\ldots,\mathbf{x}_N,\mathbf{u}_0,\ldots,\mathbf{u}_N} \quad & J\left(\mathbf{x}_k, \mathbf{u}_k\right) \\ \text{subject to} \quad & \mathbf{x}_{k+1} = \mathbf{A}\mathbf{x}_k + \mathbf{B}\mathbf{u}_k, \\ & \mathbf{x}_k \in \mathcal{X}, \mathbf{u}_k \in \mathcal{U}, \\ & \mathbf{x}_0 = \mathbf{x}\left(0\right). \end{aligned} \tag{3}$$

The question of finding optimal $\mathbf{u}$ is a quadratic program (QP) (Boyd and Vandenberghe, 2004). With the receding-horizon implementation, only the first element $\mathbf{u}(0)$ is applied as the current value of the controller output.

3 QUADRATIC PROGRAM

We use the condensed form of the QP, in which only $\mathbf{u}_k$ are assembled into the optimization variable. The $\mathbf{x}_k$-dependent terms of the cost function and the constraints on $\mathbf{x}_k$ are substituted using (1) (Ullmann and Richter, 2012).

The QP (3) can be written as:

$$\begin{aligned} \text{minimize} \quad & \frac{1}{2}\mathbf{z}^{\mathrm{T}}\mathbf{H}\mathbf{z} + \mathbf{c}^{\mathrm{T}}\mathbf{z} \\ \text{subject to} \quad & \mathbf{C}\mathbf{z} \preceq \mathbf{b}, \end{aligned} \tag{4}$$

$\mathbf{z} \in \mathbb{R}^{k \cdot m}$ is the optimization variable, constructed for example as

$$\mathbf{z} = \begin{bmatrix} \mathbf{u}_0 \\ \mathbf{u}_1 \\ \vdots \\ \mathbf{u}_N \end{bmatrix}.$$

The Hessian $\mathbf{H}$ is symmetric positive semidefinite by construction. We are particularly interested in examples with positive definite $\mathbf{H}$ which is often the case. Lagrange duality is used. Unconstrained optimization

$$\text{minimize} \quad \frac{1}{2}\mathbf{z}^{\mathrm{T}}\mathbf{H}\mathbf{z} + \mathbf{c}^{\mathrm{T}}\mathbf{z} + \mathbf{v}^{\mathrm{T}}\mathbf{C}\mathbf{z} \tag{5}$$

for constant value of vector $\mathbf{v}$ leads to the solution of a related quadratic program with different constraints (Everett, 1963)

$$\begin{aligned} \text{minimize} \quad & \frac{1}{2}\mathbf{z}^{\mathrm{T}}\mathbf{H}\mathbf{z} + \mathbf{c}^{\mathrm{T}}\mathbf{z} \\ \text{subject to} \quad & \mathbf{C}\mathbf{z} \preceq \mathbf{b}'. \end{aligned} \tag{6}$$

Lagrange multiplier $\mathbf{v}$ can be adjusted until $\mathbf{b} = \mathbf{b}'$ and the solution of (5) solves the original problem (4). Search for the correct value of Lagrange multiplier is named solving the dual problem (Boyd and Vandenberghe, 2004).

4 DUAL PROXIMAL GRADIENT METHOD ALGORITHM

The indicator function of the feasible set for $\mathbf{d} \preceq \mathbf{b}$, $g(\mathbf{d})$, is defined as:

$$g\left(\mathbf{d}\right) = \begin{cases} 0; & \mathbf{d} \preceq \mathbf{b} \\ \infty; & \text{otherwise.} \end{cases} \tag{7}$$

Its conjugate function $g^*(\mathbf{d})$ is needed as well, it is defined as

$$g^*(\mathbf{d}) = \sup_{\mathbf{z}}(\mathbf{d}^{\mathrm{T}}\mathbf{z} - g(\mathbf{z})). \tag{8}$$

The iteration scheme is best described using proximity operator

$$\text{prox}_{\psi}^{L}\left(\mathbf{d}\right) = \arg\min_{\mathbf{y}} \left(\psi\left(\mathbf{y}\right) + \frac{L}{2} \left\|\mathbf{y} - \mathbf{d}\right\|^2 \right). \tag{9}$$

The algorithm of the dual gradient method is:

$$\mathbf{y}^k = \arg\min_{\mathbf{z}} \left(\frac{1}{2}\mathbf{z}^{\mathrm{T}}\mathbf{H}\mathbf{z} + \mathbf{c}^{\mathrm{T}}\mathbf{z} + \left(\mathbf{v}^k\right)^{\mathrm{T}} \mathbf{C}\mathbf{z} \right) \tag{10}$$

$$\mathbf{v}^{k+1} = \text{prox}_{g^*}^{L}\left(\mathbf{v}^k + \mathbf{C}\mathbf{y}^k\right) \tag{11}$$

where gradient of the Lagrange dual function of the objective function in (4) is Lipschitz continuous with the constant L. The highest eigenvalue of $\mathbf{M} = \mathbf{C}\mathbf{H}^{-1}\mathbf{C}^{\mathrm{T}}$ can always be used as L (Giselsson and Boyd, 2014). By scaling $\mathbf{C}$, $L = 1$ can be achieved, so without loss of generality, $L = 1$ is assumed and notation $\text{prox}_{g^*}^{1}(\mathbf{d}) = \text{prox}_{g^*}(\mathbf{d})$ is used.

It follows from the Moreau decomposition (Rockafellar, 1970, Theorem 31.5) (Giselsson and Boyd, 2014) that the prox operator of the conjugate of an indicator function is

$$\text{prox}_{g^*}\left(\mathbf{d}\right) = \mathbf{d} - \text{prox}_{g}\left(\mathbf{d}\right). \tag{12}$$

From definition of the proximity operator it follows that $\text{prox}_{g}\left(\mathbf{d}\right)$ is the projection of $\mathbf{d}$ onto the feasible

set for $\mathbf{d} \preceq \mathbf{b}$, so it is a min operation and computationally inexpensive, rendering the whole (11) inexpensive. In addition, a closed form of the solution for (10) exists:

$$\mathbf{y}^k = -\mathbf{H}^{-1}\left(\mathbf{C}^{\mathrm{T}}\mathbf{v}^k + \mathbf{c}\right) \tag{13}$$

for every positive definite Hessian. Dual proximal gradient method can thus be practically applied to solving QPs of the form discussed above in (4).

5 RATES OF DECREASE OF RESIDUALS

We define *active* constraints in step k as those whose corresponding components of $\mathbf{v}^k$ are positive. The set of these constraints is the *active set* in step k, labelled ω^k. The vector of the positive components of $\mathbf{v}^k$ is labelled $\mathbf{v}^k[\omega^k]$. The matrix formed from the rows of $\mathbf{C}$ that correspond to active constraints is labelled $\mathbf{C}[\omega^k]$. The matrix formed from the intersections of the rows and columns corresponding to active constraints of $\mathbf{M}$ is $\mathbf{M}[\omega^k|\omega^k]$ and is a principal submatrix of $\mathbf{M}$.

Consider three iterations k, $k+1$, $k+2$ for which the active set remains constant ($\omega^k = \omega^{k+1} = \omega^{k+2} = \omega$). Let us define dual residuals

$$\begin{aligned} \Delta^k &= \mathbf{v}^{k+1} - \mathbf{v}^k \\ \Delta^{k+1} &= \mathbf{v}^{k+2} - \mathbf{v}^{k+1} \end{aligned} \tag{14}$$

and analyse the relationship between Δ^k and Δ^{k+1}.

The components of $\Delta^{k,k+1}$ that do not form $\Delta^{k,k+1}[\omega]$ are equal to 0, so it is sufficient to study $\Delta^{k,k+1}[\omega]$. Expressing Δ^k with $\mathbf{v}^k$, we get from (11):

$$\mathbf{v}^{k+1} = \mathrm{prox}_{g^*}\left(\mathbf{v}^k + \mathbf{C}\mathbf{y}^k\right) \tag{15}$$

According to (12),

$$\mathbf{v}^{k+1} = \mathbf{v}^k + \mathbf{C}\mathbf{y}^k - \mathrm{prox}_g\left(\mathbf{v}^k + \mathbf{C}\mathbf{y}^k\right). \tag{16}$$

From (13), it follows

$$\mathbf{y}^k = -\mathbf{H}^{-1}\left(\mathbf{C}^{\mathrm{T}}\mathbf{v}^k + \mathbf{c}\right). \tag{17}$$

Equations (16, 17) combine into

$$\mathbf{v}^{k+1} = \mathbf{v}^k - \mathbf{M}\mathbf{v}^k - \mathbf{C}\mathbf{H}^{-1}\mathbf{c} - \mathrm{prox}_g\left(\mathbf{v}^k + \mathbf{C}\mathbf{y}^k\right). \tag{18}$$

By definition of ω, (18) turns into

$$\mathbf{v}^{k+1}[\omega] = \left(\mathbf{v}^k - \mathbf{M}\mathbf{v}^k - \mathbf{C}\mathbf{H}^{-1}\mathbf{c} - \mathbf{b}\right)[\omega] \tag{19}$$

and

$$\mathbf{v}^{k+1}[\omega] = \mathbf{v}^k[\omega] - \mathbf{M}[\omega|\omega]\,\mathbf{v}^k[\omega] - \left(\mathbf{C}\mathbf{H}^{-1}\mathbf{c} + \mathbf{b}\right)[\omega] \tag{20}$$

follows. Definition (14) leads to

$$\Delta^k[\omega] = \mathbf{v}^{k+1}[\omega] - \mathbf{v}^k[\omega] \tag{21}$$

and (20, 21) give

$$\Delta^k[\omega] = -\mathbf{M}[\omega|\omega]\,\mathbf{v}^k[\omega] - \left(\mathbf{C}\mathbf{H}^{-1}\mathbf{c} + \mathbf{b}\right)[\omega]. \tag{22}$$

In (19) we have taken into account that $\mathrm{prox}_g(\mathbf{v}^k + \mathbf{C}\mathbf{y}^k)[\omega] = \mathbf{b}[\omega]$, following from the definition of ω.

Δ^{k+1} can be expressed with Δ^k:

$$\begin{aligned} \Delta^{k+1}[\omega] &= -\mathbf{M}[\omega|\omega]\,\mathbf{v}^{k+1}[\omega] - \left(\mathbf{C}\mathbf{H}^{-1}\mathbf{c} + \mathbf{b}\right)[\omega] \\ \Delta^{k+1}[\omega] &= -\mathbf{M}[\omega|\omega]\left(\mathbf{v}^k[\omega] + \Delta^k[\omega]\right) - \\ &\qquad \left(\mathbf{C}\mathbf{H}^{-1}\mathbf{c} + \mathbf{b}\right)[\omega] \\ \Delta^{k+1}[\omega] &= \Delta^k[\omega] - \mathbf{M}[\omega|\omega]\,\Delta^k[\omega] \\ \Delta^{k+1}[\omega] &= \left(\mathbf{I} - \mathbf{M}[\omega|\omega]\right)\Delta^k[\omega], \end{aligned} \tag{23}$$

where $\mathbf{I}$ is the identity matrix the same size as $\mathbf{M}[\omega|\omega]$.

Since $\mathbf{M}[\omega|\omega]$ is symmetric, its eigenvectors are orthogonal (Graselli, 1975, p. 83) and (23) can be conveniently diagonalized using eignedecomposition into

$$\mathbf{d}^{k+1} = (\mathbf{I} - \mathbf{D})\,\mathbf{d}^k, \tag{24}$$

where $\mathbf{D} = \mathbf{V}^{\mathrm{T}}\mathbf{M}[\omega|\omega]\mathbf{V}$, $\mathbf{d}^{k,k+1} = \mathbf{V}^{\mathrm{T}}\Delta^{k,k+1}[\omega]$, $\mathbf{V}$ is orthogonal and its columns are eignevectors of $\mathbf{M}$, $\mathbf{D}$ is diagonal with eigenvalues λ_i^ω of $\mathbf{M}[\omega|\omega]$ on the diagonal.

In each iteration, the i-th component of $\mathbf{d}^k$ gets multiplied by $1-\lambda_i^\omega$. If $0 < \lambda_i^\omega < 2$, the component is decreasing toward 0. It can be shown that the components of $\mathbf{v}^k$ that lie in the nullspace of $\mathbf{M}[\omega|\omega]$ do not affect $\mathbf{y}^k$ (see appendix) so if $\lambda_i^\omega = 0$, the corresponding component does not influence the primal solution $\mathbf{y}$. Moreover, $\mathbf{d}_i^k = 0$ for $\lambda_i^\omega = 0$ if ω is a feasible active set, as shown in the appendix. For a given ω, the qudratic norm of residual is thus decreasing toward 0 if $0 \leq \lambda_i^\omega < 2$ for every λ_i^ω. The slowest component of residual to decay corresponds to the lowest non-zero λ_i^ω, components of residual proportional to higher λ_i^ω have faster dynamics. If the ω being studied is the final active set and will not change in subsequent iterations, the lowest non-zero λ_i^ω determines the convergence rate.

From theorem 4.3.15 in (Horn and Johnson, 1990) it follows that the lowest eigenvalue of the symmetric matrix $\mathbf{M}$ forms the lower bound for eigenvalues of the principal submatrices $\mathbf{M}[\omega|\omega]$ of $\mathbf{M}$, and the highest eigenvalue of $\mathbf{M}$ is the upper bound for eigenvalues of $\mathbf{M}[\omega|\omega]$. $\mathbf{M}$ is positive semidefinite, so its lowest eigenvalue is bigger or equal to 0. It has been assumed that the highest eigenvalue of $\mathbf{M}$ is set below or equal to 1 through multiplying $\mathbf{C}$ and $\mathbf{b}$ with a positive

constant. It guarantees convergence of the method for $L = 1$. Scaling the problem influences the local rate of decrease of residual: enlarging $\mathbf{M}$ also enlarges each $\mathbf{M}[\omega|\omega]$ and its eigenvalues, among them each lowest non-zero eigenvalue that determines the local rate of decrease of the slowest component of residual.

In MPC-related practical examples, the lowest eigenvalue of $\mathbf{M}$ is typically equal to 0. The theorem is thus not sufficient to derive a positive lower bound for the lowest non-zero eigenvalue of the principal submatrices $\mathbf{M}[\omega|\omega]$. In particular, the lowest non-zero eigenvalue of a principal submatrix $\mathbf{M}[\omega|\omega]$ can be smaller than the lowest non-zero eigenvalue of $\mathbf{M}$.

It is worth noting that the vectors determining the QP do not directly influence the convergence rate other than through ω and that analysis of the matrices yields convergence rate estimates that are independent of current MPC system state and reference. Analysing eigenvalues of $\mathbf{M}[\omega|\omega]$ for various ω is sufficient.

6 PRACTICAL EXTENSIONS

6.1 Preconditioning or Generalization

Use of the generalized prox operator in place of prox operator can improve convergence (Giselsson, 2013). The generalized prox operator is defined in the following way:

$$\text{prox}_{\psi}^{\mathbf{L}_\mu}(\mathbf{d}) = \arg\min_{\mathbf{y}} \left(\psi(\mathbf{y}) + \frac{1}{2} \|\mathbf{y}-\mathbf{d}\|_{\mathbf{L}_\mu}^2 \right), \quad (25)$$

where $\mathbf{L}_\mu$ is chosen to be a diagonal positive definite matrix. (11) is modified using the generalized prox operator to obtain

$$\mathbf{v}^{k+1} = \text{prox}_{g^*}^{\mathbf{L}_\mu}\left(\mathbf{v}^k + \mathbf{C}\mathbf{y}^k\right). \quad (26)$$

Consider the following quadratic program:

$$\begin{aligned} \text{minimize} \quad & \frac{1}{2}\mathbf{z}^{\mathrm{T}}\mathbf{H}\mathbf{z} + \mathbf{c}^{\mathrm{T}}\mathbf{z} \\ \text{subject to} \quad & \tilde{\mathbf{C}}\mathbf{z} \preceq \tilde{\mathbf{b}}, \end{aligned} \quad (27)$$

where $\tilde{\mathbf{C}}$ stands for $\mathbf{EC}$ and $\tilde{\mathbf{b}}$ is $\mathbf{Eb}$, $\mathbf{E}$ being a diagonal positive definite matrix. Taking into account (Giselsson, 2013)

$$\text{prox}_{g^*}^{\mathbf{L}_\mu}(\mathbf{d}) = \mathbf{d} - \mathbf{L}_\mu^{-1}\text{prox}_{g}^{\mathbf{L}_\mu^{-1}}(\mathbf{L}_\mu\mathbf{d}) \quad (28)$$

it follows that using (10, 11) to solve (27) is equivalent to solving (4) using (10, 26) if $\mathbf{E} = \mathbf{L}_\mu^{-1}$.

The procedure of generalization or preconditioning consists of finding a suitable $\mathbf{E}$ and changing the QP in (4) into the one in (27). It is then solved using (10, 11). The matrix $\mathbf{M}$ is replaced by $\tilde{\mathbf{M}} = \tilde{\mathbf{C}}\mathbf{H}^{-1}\tilde{\mathbf{C}}^{\mathrm{T}} = \mathbf{EME}$. The highest eignevalue of $\tilde{\mathbf{M}}$ is chosen by scaling $\mathbf{E}$ and should be ≤ 1 for convergence to be guaranteed taking $L = 1$. Better choices of $\mathbf{E}$ lead to bigger lowest positive eigenvalues of the encountered $\tilde{\mathbf{M}}[\omega^k|\omega^k]$.

6.2 Upper and Lower Boundaries

In MPC, it is typical to have upper and lower bounds on the same signals, which leads to the same linear functionals of the optimization variable in QP having both upper and lower bounds as well. If the QP is given in the form of (4), $\mathbf{C}$ can thus be written as:

$$\mathbf{C} = \begin{bmatrix} \mathbf{C}_1 \\ -\mathbf{C}_1 \end{bmatrix}. \quad (29)$$

Then inequality (4) can be reformulated as

$$\mathbf{b}_1 \preceq \mathbf{C}_1\mathbf{z} \preceq \mathbf{b}_2. \quad (30)$$

In the computational code, $\mathbf{C}$ is replaced with $\mathbf{C}_1$, resulting in smaller matrices (among them $\mathbf{M}$) and in halving the length of Lagrange multiplier, the same component now corresponding to both the upper and the lower boundary depending on its sign. It follows that $g(\mathbf{d})$ becomes the indicator function of the feasible set for $\mathbf{b}_1 \preceq \mathbf{d} \preceq \mathbf{b}_2$. It causes $\text{prox}_g(\mathbf{d})$ to turn into projection onto a box that can be implemented using a min and a max operation.

The modification does not change theoretical behaviour of the system but lowers the computational needs. Importantly, rewriting (4) in the form of (29) halves the size of $\mathbf{M}$ while keeping the same eigenvalues of $\tilde{\mathbf{M}}[\omega|\omega]$ and preserving the relationship between $\tilde{\mathbf{M}}[\omega|\omega]$ and local rate of decrease of residual.

6.3 Soft Constraints

QP resulting from MPC problem with state constraints may not be feasible, meaning it does not necessarily have a solution. However, in practice we want the controller to produce a sensible output $\mathbf{u}$ also when the constraints cannot be satisfied. One way of doing it is relaxing the inequality state constraints from (4) with a slack variable which is penalized in the cost function. The QP expands to the form:

$$\begin{aligned} \text{minimize} \quad & \frac{1}{2}\mathbf{z}^{\mathrm{T}}\mathbf{H}\mathbf{z} + \mathbf{c}^{\mathrm{T}}\mathbf{z} + \mathbf{w}^{\mathrm{T}}\mathbf{s} \quad (31) \\ \text{subject to} \quad & \mathbf{C}\mathbf{z} \preceq \mathbf{b} + \mathbf{s}, \quad (32) \end{aligned}$$

where $\mathbf{s} \in \mathbb{R}_+^n$ is the slack variable, and $\mathbf{w} \in \mathbb{R}_+^n \cup \infty$ is its weight (Giselsson, 2013; Kouzoupis, 2014). If the QP in (4) has a feasible solution and if the weight $\mathbf{w}$

is big enough, the solution of the new problem is the solution of the original QP and $\mathbf{s} = \mathbf{0}$. For smaller $\mathbf{w}$ or for infeasible QP, $\mathbf{s}$ has non-zero components.

A way to efficiently implement soft constraints with linear cost of constraint violation can be seen by comparing (5) to (31). If $\mathbf{w}$ is taken to be the upper bound for Lagrange multipliers $\mathbf{v}$, dual proximal gradient method solves the soft-constrained problem. The components of the dual residual corresponding to the violated soft constraints are 0, thus violated soft state constraints appear among inactive constraints when calculating the local rate of decrease of residual.

7 EXAMPLE

A discrete-time form of the AFTI-16 benchmark model as in (Giselsson, 2013) has the system matrices

$$\mathbf{A} = \begin{bmatrix} 0.9993 & -3.0083 & -0.1131 & -1.6081 \\ -0.0000 & 0.9862 & 0.0478 & 0.0000 \\ 0.0000 & 2.0833 & 1.0089 & -0.0000 \\ 0.0000 & 0.0526 & 0.0498 & 1.0000 \end{bmatrix}$$

$$\mathbf{B} = \begin{bmatrix} -0.0804 & -0.6347 \\ -0.0291 & -0.0143 \\ -0.8679 & -0.0917 \\ -0.0216 & -0.0022 \end{bmatrix}$$

in (1). The constraints are:

$$\begin{aligned} \mathcal{X} &= \{\mathbf{x} \in \mathbb{R}^4; -0.5 - s_1 \leq x_2 \leq 0.5 + s_1, \\ &\quad -100 - s_2 \leq x_4 \leq 100 + s_2\} \\ \mathcal{U} &= \{\mathbf{u} \in \mathbb{R}^2; -25 \leq u_1 \leq 25, \\ &\quad -25 \leq u_2 \leq 25\}. \end{aligned} \tag{33}$$

The constraints on the components of $\mathbf{x}$ are soft, linear weight on the components of the slack is $\mathbf{w} = [10^5, 10^5]^{\mathrm{T}}$ and $\mathbf{w}^{\mathrm{T}}\mathbf{s}(k)$ is added to the sum term in (2). The cost matrices are

$$\mathbf{Q} = \mathrm{diag}(10^{-4}, 10^2, 10^{-3}, 10^2), \quad \mathbf{R} = \mathrm{diag}(10^{-2}, 10^{-2}) \tag{34}$$

The reference $\mathbf{x_r}$ is 0 in all components except for the first 50 time steps of the simulation, where for x_4 it is 10. Initial state at the beginning of the simulation is $\mathbf{x}(0) = [0,0,0,0]^{\mathrm{T}}$

A family of QP in condensed form (4) corresponding to the MPC problem is formed for $N = 10$ using *QPgen* (QPgen, 2014; Giselsson and Boyd, 2014). The matrices $\mathbf{C}$ and $\mathbf{H}$ are constant while the vectors $\mathbf{b}$ and $\mathbf{c}$ are dependent on the system state and the reference. The QPs are 20-dimensional (10 x 2 components of $\mathbf{u}$) with 40 lines in $\mathbf{C}$ (limits on 10 x 2 input signals and 10 x 2 state components).

The preconditioning diagonal matrix $\mathbf{E}$ is chosen so as to minimize the condition number of the non-singular part of $\mathbf{M}$ while setting the highest eigenvalue of $\mathbf{M}$ to 1. *QPgen* finds $\mathbf{E} = \mathrm{diag}(10.4796,$ 3.5413, 9.9973, 10.0080, 9.9987, 10.0005, 10.0000, 10.0037, 9.9990, 9.9997, 10.0001, 10.0033, 9.9989, 9.9979, 10.0003, 10.0036, 9.9999, 9.9965, 9.9972, 10.0034, 0.2058, 0.0918, 0.1003, 0.1000, 0.1007, 0.1001, 0.1005, 0.1000, 0.1004, 0.1001, 0.1007, 0.1000, 0.1004, 0.1001, 0.1009, 0.0999, 0.1004, 0.1000, 0.1013, 0.1000). The model is initially simulated in closed loop with 10^6 iterations in every time step for 100 time steps. The system state $\mathbf{x}$ is recorded at every time step and used as the input initial state for observing convergence of the QP. Algorithm behaviour is analysed in all time steps for 1 to 3000 iterations.

Figure 1 shows the active sets through iterations for the first 10 time steps. White columns are delimiters of time steps.

In Figure 2, convergence through active set changes in time step 1 is shown graphically. Firstly we analyse the behaviour with the final ω. The quadratic norm of the primal residual is 0.22805 in 300th iteration and 8.74325×10^{-12} in 1800th iteration, so the difference gets multiplied by 0.98414 in each iteration. This gives the estimate for the smallest non-zero eigenvalue of the relevant $\mathbf{M}[\omega|\omega]$ of $1 - 0.98414 = 0.01586$. In fact, 20 constraints are active during the considered iterations (and no soft ones are violated), 9 of them soft corresponding to state constraints and 11 hard corresponding to input constraints. The matrix $\mathbf{M}[\omega|\omega]$ is non-singular and its lowest eigenvalue is 0.01587, showing good agreement with the numerical behaviour.

There is another longer interval in the first sample where the active set does not change between 24th and 153th iteration. The set has 22 elements, 9 of which are soft constraints and 13 are hard, no constraint is violated. If the dual residual is transformed into the eigenspace of $\mathbf{M}[\omega|\omega]$, one expects the components to decay in proportion with their corresponding eigenvalues of M. In Figure 3, these components are plotted. It can be seen that the 22 lines decay with different slopes in the relevant region and that the ones listed higher in the legend decay slower – they are listed in ascending order with respect to eigenvalues (the first 2 correspond to the eigenvalues that are 0 and stay constant). Similarly, the active set is constant from 161th iteration on, has 20 elements, and $\mathbf{M}[\omega|\omega]$ has no eigenvalues equal to 0. The corresponding eigendecomposition of the dual residual is shown in Figure 4.

Similar results for the time step 76 are shown in

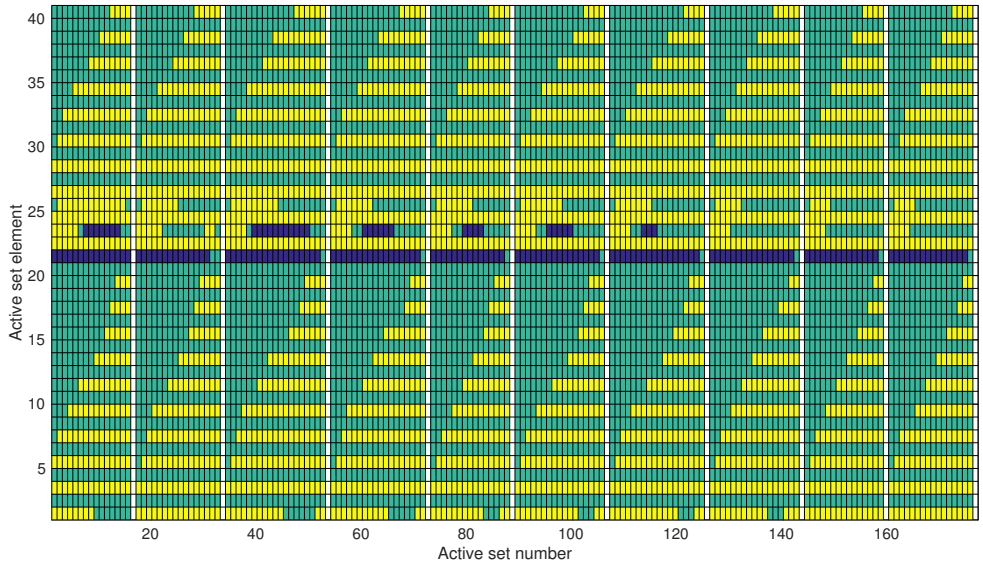

Figure 1: The list of active sets for the first 10 samples. The constraints are listed from the bottom to the top, the first 20 correspond to the input constraints on **u** from 1st to *N*th time step, the following 20 are from constraints on **x**, again for 10 steps. Samples are listed from left to right, white columns separate them. For a given sample, the first active set is on the left and every change of the active set results in a new column. Yellow fields mean active upper limit constraint, blue fields are for the lower limit, green ones are inactive constraints or violated soft constraints.

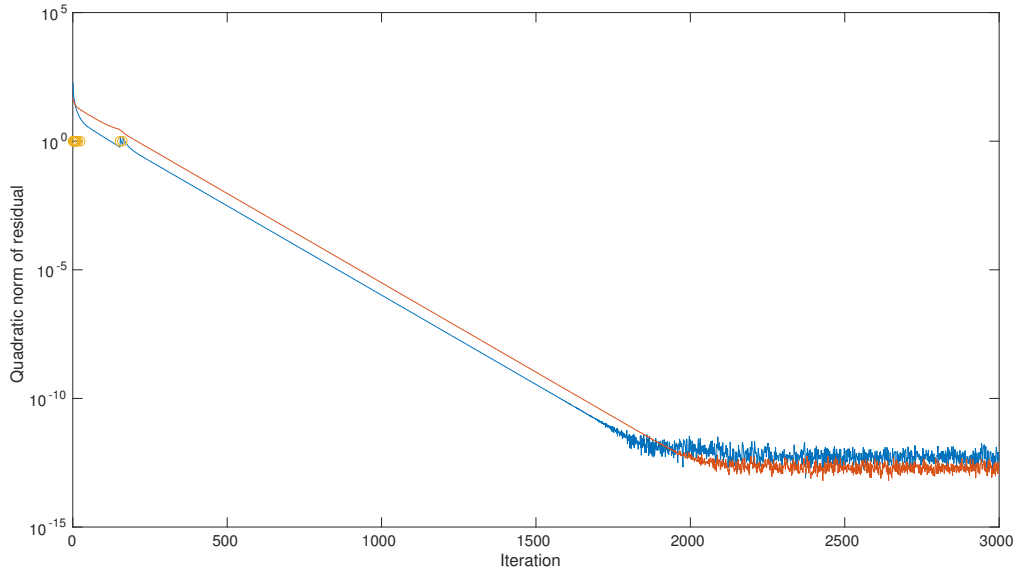

Figure 2: Convergence of the quadratic norm of the primal (blue) and the dual (red) solution in time step 1 as a function of the iteration number. The yellow circles mark iterations in which the active set changes.

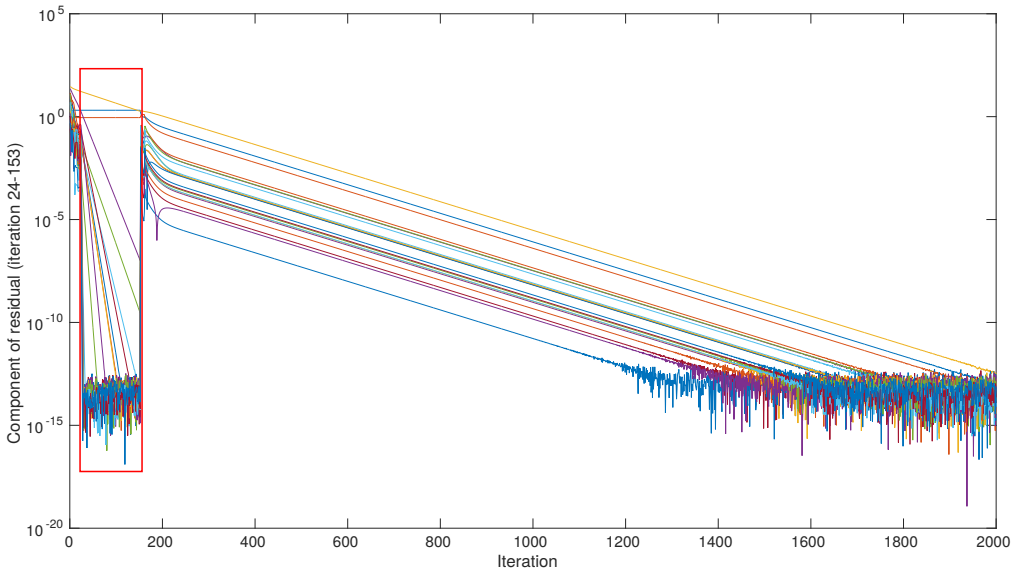

Figure 3: The components of the dual residual parallel to eigenvectors of $\mathbf{M}[\omega|\omega]$ between iterations 24 and 153 (red frame) for time step 1 as a function of the iteration number. The components are listed in the order of ascending corresponding eigenvalues.

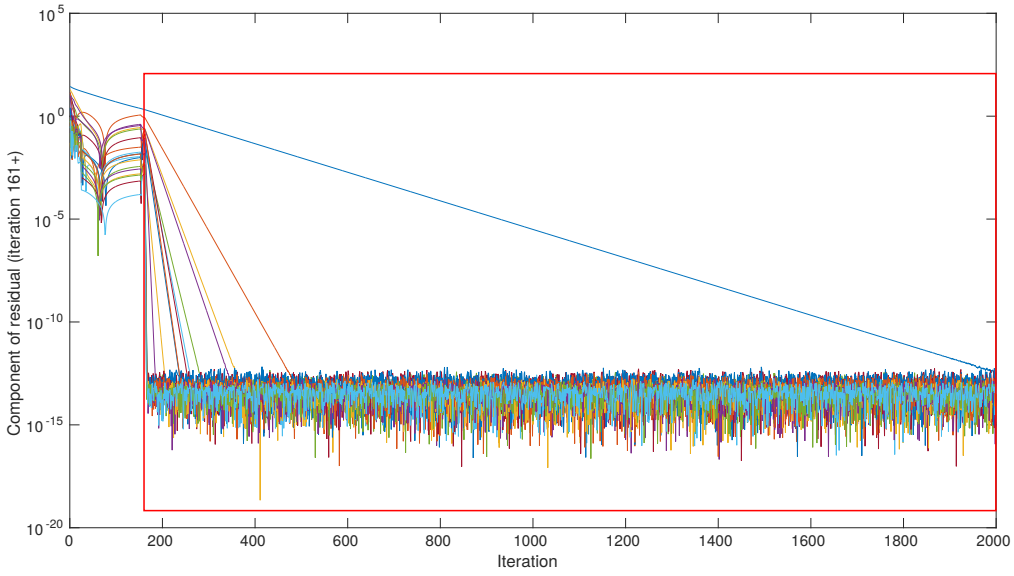

Figure 4: The components of the dual residual parallel to eigenvectors of $\mathbf{M}[\omega|\omega]$ from iteration 161 on (red frame) for time step 1 as a function of the iteration number. The components are listed in the order of ascending corresponding eigenvalues.

Figures 5 and 6. For the majority of iterations, ω has 4 elements and the lowest eigenvalue of $\mathbf{M}[\omega|\omega]$ is 0.1266 so convergence is faster than in time step 1.

8 CONCLUSION

The local rate of decrease of residuals for dual gradient method is explained. For an active set ω, it is limited by the lowest non-zero eigenvalue of $\mathbf{M}[\omega|\omega]$. The problem of certification can thus be seen as seeking a lower bound for non-zero eigenvalues of $\mathbf{M}[\omega|\omega]$.

In further work, we intend to test lower bounds of as many active sets as possible, although it is generally known that this problem is plagued with combinatorial complexity. We will also try to extend the approach to the fast dual gradient method without and with restarting and use the results in the preconditioning phase to speed up convergence.

ACKNOWLEDGEMENTS

Research supported by Slovenian Research Agency (P2-0001). This work has been carried out within the framework of the EUROfusion Consortium and has received funding from the Euratom research and training programme 2014-2018 under grant agreement No 633053. The views and opinions expressed herein do not necessarily reflect those of the European Commission.

REFERENCES

Boyd, S. and Vandenberghe, L. (2004). *Convex Optimization*. Cambridge University Press, New York, NY, USA.

Domahidi, A., Zgraggen, A. U., Zeilinger, M. N., Morari, M., and Jones, C. (2012). Efficient Interior Point Methods for Multistage Problems Arising in Receding Horizon Control. In *Proceedings of the 51st IEEE Conference on Decision and Control*.

Everett, H. (1963). Generalized lagrange multiplier method for solving problems of optimum allocation of resources. *Oper. Res.*, 11(3):399–417.

Ferreau, H. J., Bock, H. G., and Diehl, M. (2008). An online active set strategy to overcome the limitations of explicit MPC. *International Journal of Robust and Nonlinear Control*, 18(8):816–830.

Ferreau, H. J., Kirches, C., Potschka, A., Bock, H. G., and Diehl, M. (2014). qpoases: a parametric active-set algorithm for quadratic programming. *Math. Program. Comput.*, 6(4):327–363.

Gerkšič, S. and Tommasi, G. D. (2014). Improving magnetic plasma control for ITER. *Fusion Engineering and Design*, 89(910):2477 – 2488. Proceedings of the 11th International Symposium on Fusion Nuclear Technology-11 (ISFNT-11) Barcelona, Spain, 15-20 September, 2013.

Giselsson, P. (2013). Improving Fast Dual Ascent for MPC - Part II: The Embedded Case. *ArXiv e-prints*.

Giselsson, P. and Boyd, S. (2014). Preconditioning in fast dual gradient methods. In *53rd IEEE Conference on Decision and Control, CDC 2014, Los Angeles, CA, USA, December 15-17, 2014*, pages 5040–5045.

Giselsson, P. and Boyd, S. (2015). Metric selection in fast dual forward-backward splitting. *Automatica*, 62:1–10.

Graselli, J. (1975). Linearna algebra. In *Višja matematika II*. Državna založba Slovenije, Ljubljana, Slovenija.

Hartley, E. N., Jerez, J. L., Suardi, A., Maciejowski, J. M., Kerrigan, E. C., and Constantinides, G. A. (2014). Predictive control using an FPGA with application to aircraft control. *IEEE Trans. Control Systems Technology*, 22(3).

Horn, R. A. and Johnson, C. R. (1990). *Matrix Analysis*. Cambridge University Press.

Kapasouris, P., Athans, M., and Stein, G. (1990). Design of feedback control systems for unstable plants with saturating actuators. In *Proceedings of the IFAC Symposium on Nonlinear Control System Design*, page 302 307. Pergamon Press.

Kouzoupis, D. (2014). *Complexity of First-Order Methods for Fast Embedded Model Predictive Control (Master Thesis)*. Eidgenssische Technische Hochschule, Zrich.

Mattingley, J. and Boyd, S. (2012). CVXGEN: a code generator for embedded convex optimization. *Optimization and Engineering*, 13(1):1–27.

Mattingley, J., Wang, Y., and Boyd, S. (2011). Receding horizon control, automatic generation of high-speed solvers. *IEEE Control Syst. Mag.*, 31:52 –65.

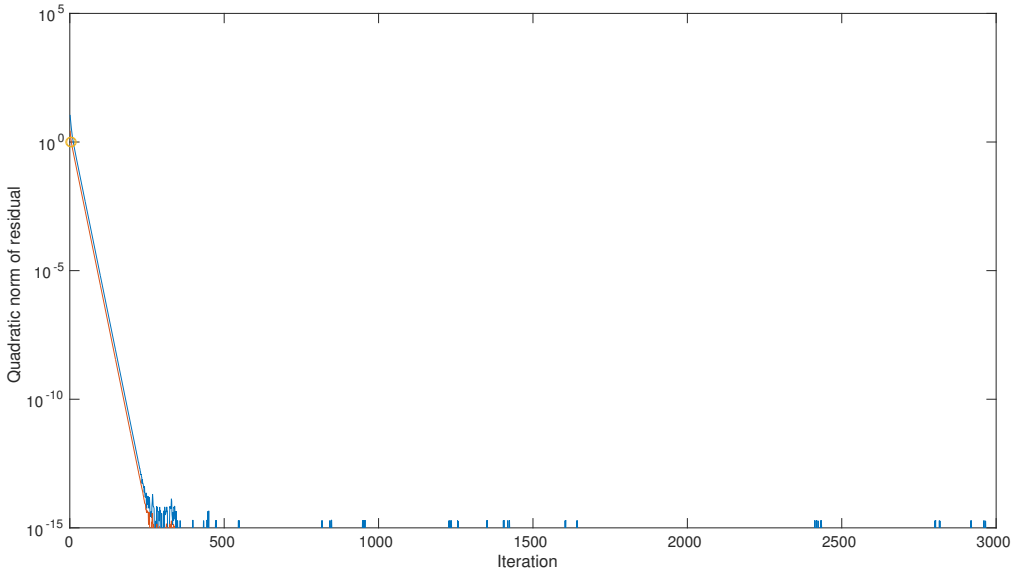

Figure 5: The quadratic norm of the primal (blue) and the dual (red) residual in time step 76 as a function of the iteration number. The yellow circles mark iterations in which the active set changes.

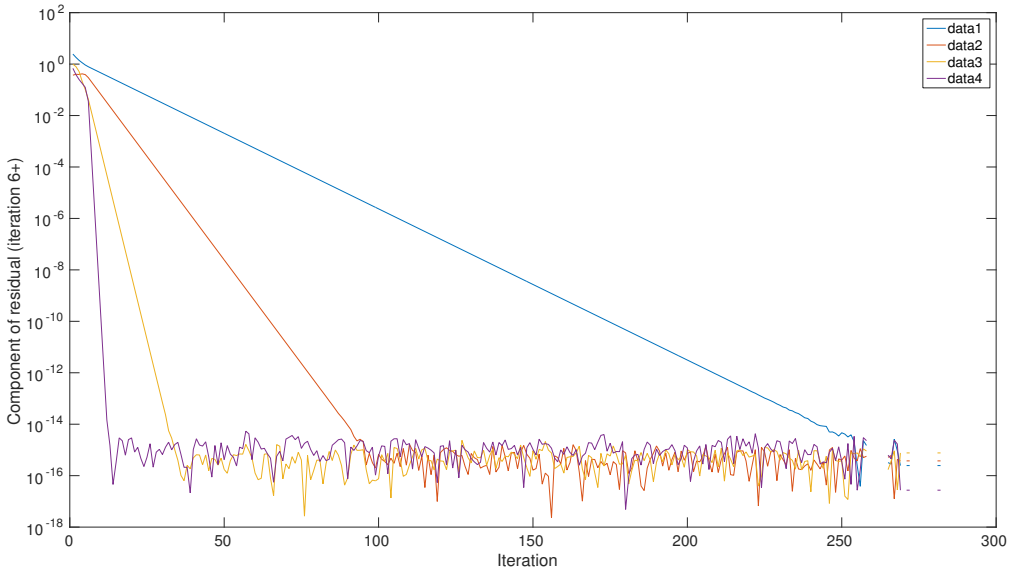

Figure 6: The components of the dual residual parallel to eigenvectors of $\mathbf{M}[\omega|\omega]$ from iteration 6 on for time step 76 as a function of the iteration number. The components are listed in the order of ascending corresponding eigenvalues.

Patrinos, P., Guiggiani, A., and Bemporad, A. (2015). A dual gradient-projection algorithm for model predictive control in fixed-point arithmetic. *Automatica*, 55(C):226–235.

Qin, S. and Badgwell, T. A. (2003). A survey of industrial model predictive control technology. *Control Engineering Practice*, 11(7):733 – 764.

QPgen (2014). QPgen. Accessed 24 January 2017.

Richter, S. (2012). *Computational Complexity Certification of Gradient Methods for Real-Time Model Predictive Control (Dissertation)*. Eidgenssische Technische Hochschule, Zrich.

Rockafellar, R. T. (1970). *Convex Analysis*. Princeton University Press, Princeton, New Jersey.

Ullmann, F. and Richter, S. (2012). *FiOrdOs – MPC Example*. Automatic Control Laboratory, ETH Zurich, Zurich.

Wang, Y. and Boyd, S. (2010). Fast model predictive control using online optimization. *IEEE Trans Control Syst Techn*, 18:267–278.

APPENDIX

Components of $\mathbf{v}^k$ Corresponding to Nullspace of $\mathbf{M}[\omega|\omega]$ Do Not Influence $\mathbf{y}^k$

Let $\mathbf{M}[\omega|\omega]\mathbf{v}^{\omega}[\omega] = 0$. By definition, $\mathbf{M}[\omega|\omega] = \mathbf{C}[\omega]\mathbf{H}^{-1}(\mathbf{C}[\omega])^{\mathrm{T}}$. Since $\mathbf{H}^{-1}$ is positive definite, $\mathbf{z}^{\mathrm{T}}\mathbf{H}^{-1}\mathbf{z} > 0$ for every $\mathbf{z}$ different from 0 (Graselli, 1975, p. 90). Let $\mathbf{z} = (\mathbf{C}[\omega])^{\mathrm{T}}\mathbf{v}^{\omega}[\omega]$. Then $0 = (\mathbf{v}^{\omega}[\omega])^{\mathrm{T}}\mathbf{M}[\omega|\omega]\mathbf{v}^{\omega}[\omega] = (\mathbf{v}^{\omega}[\omega])^{\mathrm{T}}\mathbf{C}[\omega]\mathbf{H}^{-1}(\mathbf{C}[\omega])^{\mathrm{T}}\mathbf{v}^{\omega}[\omega] = \mathbf{z}^{\mathrm{T}}\mathbf{H}^{-1}\mathbf{z}$. Thus $\mathbf{z} = (\mathbf{C}[\omega])^{\mathrm{T}}\mathbf{v}^{\omega}[\omega] = 0$. According to (13), addition of $\mathbf{v}^{\omega}[\omega]$ to $\mathbf{v}^k[\omega]$ does not affect $\mathbf{y}^k$.

Dual Residual Is Perpendicular to Nullspace of $\mathbf{M}[\omega|\omega]$ for Feasible ω

If the definition of $\mathbf{M}[\omega|\omega]$ is taken into account in 22, it follows:

$$\Delta^k[\omega] = -\mathbf{C}[\omega]\mathbf{H}^{-1}(\mathbf{C}[\omega])^{\mathrm{T}}\mathbf{v}^k[\omega] - \mathbf{C}[\omega]\mathbf{H}^{-1}\mathbf{c} - \mathbf{b}[\omega]. \tag{35}$$

Let $\mathbf{t}$ be a vector from nullspace of $\mathbf{M}[\omega|\omega]$. Taking the result from the previous appendix into account, it follows $(\mathbf{C}[\omega])^{\mathrm{T}}\mathbf{t} = 0$. Next, we calculate:

$$\begin{aligned}
\mathbf{t}^{\mathrm{T}}\Delta^k[\omega] &= -\mathbf{t}^{\mathrm{T}}\mathbf{C}[\omega]\mathbf{H}^{-1}(\mathbf{C}[\omega])^{\mathrm{T}}\mathbf{v}^k[\omega] - \mathbf{t}^{\mathrm{T}}\mathbf{C}[\omega]\mathbf{H}^{-1}\mathbf{c} - \mathbf{t}^{\mathrm{T}}\mathbf{b}[\omega] \\
&= -\left((\mathbf{C}[\omega])^{\mathrm{T}}\mathbf{t}\right)^{\mathrm{T}}\mathbf{H}^{-1}(\mathbf{C}[\omega])^{\mathrm{T}}\mathbf{v}^k[\omega] \\
&\quad -\left((\mathbf{C}[\omega])^{\mathrm{T}}\mathbf{t}\right)^{\mathrm{T}}\mathbf{H}^{-1}\mathbf{c} - \mathbf{t}^{\mathrm{T}}\mathbf{b}[\omega] \\
&= -\mathbf{t}^{\mathrm{T}}\mathbf{b}[\omega].
\end{aligned}$$

If ω is a feasible active set, there exists a vector $\mathbf{u}$ so that $\mathbf{C}[\omega]\mathbf{u} = \mathbf{b}[\omega]$. Thus

$$\mathbf{t}^{\mathrm{T}}\Delta^k[\omega] = -\mathbf{t}^{\mathrm{T}}\mathbf{C}[\omega]\mathbf{u} = -\left((\mathbf{C}[\omega])^{\mathrm{T}}\mathbf{t}\right)^{\mathrm{T}}\mathbf{u} = 0. \tag{36}$$

An arbitrary vector $\mathbf{t}$ from the nullspace of $\mathbf{M}[\omega|\omega]$ is orthogonal to $\Delta^k[\omega]$, so $\Delta^k[\omega]$ is orthogonal to the nullspace of $\mathbf{M}[\omega|\omega]$.